Inorganic Chemistry

Article

pubs.acs.org/IC

Peptide Bond Hydrolysis Catalyzed by the Wells–Dawson $Zr(\alpha_2\text{-}P_2W_{17}O_{61})_2$ Polyoxometalate

Gregory Absillis and Tatjana N. Parac-Vogt*

Department of Chemistry, KU Leuven, Celestijnenlaan 200F, B-3001 Leuven, Belgium

Supporting Information

ABSTRACT: In this paper we report the first example of peptide hydrolysis catalyzed by a polyoxometalate complex. A series of metal-substituted Wells–Dawson polyoxometalates were synthesized, and their hydrolytic activity toward the peptide bond in glycylglycine (GG) was examined. Among these, the Zr(IV)- and Hf(IV)-substituted ones were the most reactive. Detailed kinetic studies were performed with the Zr(IV)-substituted Wells–Dawson type polyoxometalate $K_{15}H[Zr(\alpha_2\text{-}P_2W_{17}O_{61})_2]\cdot 25H_2O$ which was shown to act as a catalyst for the hydrolysis of the peptide bond in GG. The speciation of $K_{15}H[Zr(\alpha_2\text{-}P_2W_{17}O_{61})_2]\cdot 25H_2O$ which is highly dependent on the pD, concentration, and temperature of the solution, was fully determined with the help of ^{31}P NMR spectroscopy and its influence on the GG hydrolysis rate was examined. The highest reaction rate (k_{obs} = 9.2 (±0.2) × 10^{-5} min^{-1}) was observed at pD 5.0 and 60 °C. A 10-fold excess of GG was hydrolyzed in the presence of $K_{15}H[Zr(\alpha_2\text{-}P_2W_{17}O_{61})_2]\cdot 25H_2O$ proving the principles of catalysis. ^{13}C NMR data suggested the coordination of GG to the Zr(IV) center in $K_{15}H[Zr(\alpha_2\text{-}P_2W_{17}O_{61})_2]\cdot 25H_2O$ via its N-terminal amine group and amide carbonyl oxygen. These findings were confirmed by the inactivity of $K_{15}H[Zr(\alpha_2\text{-}P_2W_{17}O_{61})_2]\cdot 25H_2O$ toward the N-blocked analogue acetamidoglycylglycinate and the inhibitory effect of oxalic, malic, and citric acid. Triglycine, tetraglycine, and pentaglycine were also fully hydrolyzed in the presence of $K_{15}H[Zr(\alpha_2\text{-}P_2W_{17}O_{61})_2]\cdot 25H_2O$ yielding glycine as the final product of hydrolysis. $K_{15}H[Zr(\alpha_2\text{-}P_2W_{17}O_{61})_2]\cdot 25H_2O$ also exhibited hydrolytic activity toward a series of other dipeptides.

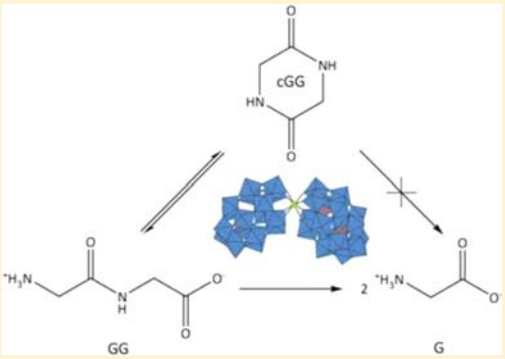

INTRODUCTION

Polyoxometalates (POMs) are a versatile class of metal–oxygen clusters endowed with a diverse range of chemical and physical properties that can be easily modified.[1] Their size, shape, composition, charge density, solubility, redox potential, and acid strength can be tuned depending on the type of application. As a consequence they are widely studied in different scientific domains such as catalysis, material science, and medicine.[2,3] Their strong Brønsted acidity and rich redox chemistry enable POMs to act as homogeneous and heterogeneous acid, redox, and bifunctional catalysts.[4] Whereas early research was traditionally focused on Brønsted acid catalysis and selective oxidation by nonsubstituted POMs, nowadays the use of metal-substituted POM derivatives as catalysts has become a quickly emerging field. By replacing one or more addenda atoms by a specific metal center, a POM with a customized coordination chemistry and reactivity is obtained. The most commonly studied type of reactions are H_2O_2-based epoxidation and sulfoxidation catalyzed by metal-substituted POMs.[5−7] For example, the di-iron substituted Keggin type silicotungstate $[\gamma\text{-}SiW_{10}(Fe(OH_2))_2O_{38}]^{6-}$, which is structurally related to the active site of methane monooxygenase, was shown to catalyze the selective epoxidation of olefins and alkanes with high H_2O_2 efficiency.[8,9] Another commercially important reaction is the synthesis of cyclic carbonates from CO_2 and epoxide.[10,11] Studies indicated that without the use of additional organic solvents and additives transition metal-substituted POMs were efficient catalysts for cyclic carbonate synthesis.[12] The use of the iron-substituted $[Fe_4(H_2O)_{10}(\beta\text{-}XW_9O_{33})_2]^{n-}$ complex as an inorganic alternative to organic and organometallic coordination complexes for the bioinspired oxygenation of catechols was demonstrated in 2009.[13] Water splitting was achieved in the presence of a tetraruthenium $[(Ru_4O_4(OH)_2(H_2O)_4(\gamma\text{-}SiW_{10}O_{36})_2]^{10-}$ complex.[14] H_2O_2-based oxidation of organic substrates was observed in the presence of Zr(IV),[15−17] Hf(IV),[17] and Ti(IV)[16] substituted POMs. Furthermore, Zr(IV)[18,19] and Hf(IV)[19] based POMs were reported as catalysts for the oxidation of sulfides. Metal-substituted POMs were also proven to be efficient catalysts for Lewis-acid mediated reactions. In 2006 the Wells–Dawson polyoxotungstate $(TBA)_5H_2[\alpha_1\text{-}Ln(H_2O)_4\text{-}P_2W_{17}O_{61}]$ (Ln = La, Sm, Eu, and Yb) was shown to be an active catalyst for aldol reactions of imines.[20] An increase in Lewis acidity compared to the Ln analogues was observed for $(TBA)_5K[\alpha_1\text{-}Hf(H_2O)_4\text{-}P_2W_{17}O_{61}]$ in Mukaiyama aldol and Mannich-type additions.[21] Efficient chemo- and diasterioselective Lewis acid catalysis was observed for the cyclization of citronellal derivatives by the dialuminium substituted silicotungstate $(TBA)_3H[\gamma\text{-}SiW_{10}O_{36}(Al(OH)_2)(\mu\text{-}OH)_2]$.[22] This study was extended to

Received: June 26, 2012
Published: August 28, 2012

   dx.doi.org/10.1021/ic301364n | Inorg. Chem. 2012, 51, 9902–9910

tetranuclear Zr(IV) and Hf(IV) sandwich type silicotungstates.[23]

Within our lab the use of POMs as catalysts for the hydrolysis of biologically relevant molecules was established some years ago. It was shown that isopolyoxomolybdates and isopolyvanadates were able to hydrolyze the phospho(di)ester bonds in a series of DNA- and RNA-model compounds.[24−30] The hydrolysis of carboxyl esters has also been achieved in the presence of oxovanadates.[31] In our recent studies we also show that peptides with a X-Ser sequence were effectively hydrolyzed in oxomolybdate and oxovanadate solutions.[32] Although hydrolysis occurred in solutions containing polyoxo forms of molybdate and vanadate, the kinetic experiments and density functional theory (DFT) calculations revealed that the actual active species are the monomeric oxoanions.[32]

In our quest to further exploit POMs as catalysts for peptide bond hydrolysis we examined the reactivity of metal-functionalized Wells−Dawson POMs toward the dipeptide glycylglycine. Metal-functionalized POMs have been shown to interact specifically with the surface of proteins, for example, the molecular interaction with albumin proteins has been studied in detail.[33] However, to the best of our knowledge the hydrolysis of the peptide bonds in the presence of POMs has not been reported so far.

The hydrolysis of the peptide bond, which is one of the most important and most required procedures in biotechnology, is a challenging task. At pH 6.8 and 25 °C, the half-life for amide bond hydrolysis in the dipeptide glycylglycine is estimated to be around 350 years.[34] Proteolytic enzymes and chemical reagents are currently used to effect protein cleavage in proteomics applications.[35] However, they both suffer from some serious shortcomings. Proteolytic enzymes tend to cleave the protein at too many sites resulting in the formation of fragments which are too short to be accurately assigned to the protein in question. Furthermore, they contaminate protein digests and often require denaturation of the protein which leads to a loss of structural information. Chemical agents, among which cyanogen bromide is the best known, usually operate under harsh conditions, have to be used in a high molecular excess, give low yields, and only exhibit partial selectivity. Clearly, new chemical reagents with improved selectivity and efficiency are needed to comply with the increasing demand in the fields of proteomics and biotechnology. Although several metal ions and complexes, including Pd(II),[36] Pt(II),[37] Ni(II),[38] Cu(II),[39] Zr(IV),[40] Zn(II),[41] Co(III),[42] and Ce(IV)[43] have been reported to promote the hydrolytic cleavage of unactivated amide bonds in peptides and proteins, the number of metal complexes that are able to catalyze peptide bond hydrolysis remains scarce.

The high Lewis acidity of Zr(IV) imparted by the +IV oxidation state, combined with its oxophilicity, kinetic lability, fast ligand-exchange kinetics, and formation of complexes with flexible geometries and high coordination numbers, makes Zr(IV) especially suitable for the hydrolysis of the amide bond in peptides and proteins. However, above pH 5.0, aqueous solutions of Zr(IV) tend to form insoluble gels and precipitates, often resulting in low hydrolysis yields.[43] To overcome this problem complexation of Zr(IV) with the azacrown ether 4,13-diaza-18-crown-6 was used in studies reported by Grant and coworkers.[40,44] This resulted in faster peptide bond hydrolysis, however, despite the reactivity increase, the formation of insoluble gels was still observed.

In our recent study we have shown that incorporation of Zr(IV) into the Wells−Dawson POM resulted in a catalyst for the homogeneous hydrolysis of phosphoesters.[45] In this study we further exploit the reactivity of Zr(IV)-POMs and report on a conceptually new approach toward the development of artificial peptidases by using the Wells−Dawson POM as a ligand for Zr(IV). We envision that the use of a POM as a chelating agent for Zr(IV) will not only result in a homogeneous reaction mixture, but may also benefit from the protein binding properties of the POM in future experiments involving the hydrolysis of proteins. To explore the potential of this novel type of reactivity, in this paper we report on the hydrolysis of several peptides and present a detailed kinetic study of glycylglycine hydrolysis by the previously reported compound $K_{15}H[Zr(\alpha_2\text{-}P_2W_{17}O_{61})_2]\cdot 25H_2O$[46] (**1**).

EXPERIMENTAL SECTION

Materials. The metal-substituted POMs were synthesized according to the procedure described in literature.[46−48] Glycylglycine, glycine anhydride, glycylglycyl amide, triglycine, tetraglycine, and pentaglycine were purchased from Sigma-Aldrich or Bachem and were used without any further purification. Acetamidoglycylglycinate[49] and ethyl glycylglycinate[50] were synthesized according to the procedure described in literature.

Sample Preparation. 2.0 mM dipeptide and 2.0 mM $K_{15}H[Zr(\alpha_2\text{-}P_2W_{17}O_{61})_2]\cdot 25H_2O$ were dissolved in D_2O and the pD value was adjusted with DCl and NaOD. The pH-meter reading was corrected by the equation: pD = pH-meter reading + 0.41.[51] $K_{15}H[Zr(\alpha_2\text{-}P_2W_{17}O_{61})_2]\cdot 25H_2O$ was not allowed to reach its equilibrium distribution before the addition of the dipeptide. The reaction was kept at 60 °C and followed at different time increments by ^{1}H NMR. Between consecutive measurements, the NMR tube was kept at 60 °C. After complete hydrolysis of the dipeptide, the pD was measured again. Typically, a value $pD_{initial} \pm 0.2$ was obtained. The decrease of the percentage of the dipeptide was fitted to a monoexponential function, and the error was calculated to be in the range of 2−7%.

NMR Spectroscopy. ^{1}H NMR spectra were recorded on a Bruker Avance 400 (SW = 12.11 ppm, TD = 32768) and Bruker Avance 600 (SW = 20.55 ppm, TD = 65536) spectrometer. As a reference 0.5 mM 3-(Trimethylsilyl)propionic-2,2,3,3-d_4 acid was present in the reaction mixture. ^{13}C NMR spectra were recorded on a Bruker Avance 400 (100.61 MHz, SW = 238.90 ppm, TD = 32768) and a Bruker Avance 600 (150.90 MHz, SW = 238.92 ppm, TD = 32768) spectrometer. As a reference 1% TMS in $CDCl_3$ in an internal reference tube was used. ^{31}P NMR spectra were recorded on a Bruker Avance 400 (161.98 MHz, SW = 399.62, TD = 65536) and a Bruker Avance 600 (242.94 MHz, SW = 395.82 ppm, TD = 65536) spectrometer. As a reference 25% H_3PO_4 in D_2O in an internal reference tube was used. The spectra were recorded at 298 K on a 5 mm PABBI 1H-BB Z-GRD and BBO 600 MHz S3 5 mm with Z-gradient; BTO probe for respectively the 400 and 600 MHz instrument.

RESULTS AND DISCUSSION

Metal-Substituted Wells−Dawson POMs. Several metal-substituted Wells−Dawson type POMs containing Mn(III), Fe(III), Co(II), Ni(II), Cu(III), Y(III), La(III), Eu(III), Yb(III), Zr(IV), and Hf(IV) were synthesized, and their reactivity toward peptide bond hydrolysis of glycylglycine (GG) was examined. After prolonged reaction times and in the presence of an excess of the metal-substituted POM only POMs containing Zr(IV) and Hf(IV) showed significant activity (1:1 POM:GG, 2.0 mM, 50 °C, pD 7.2 for Y(III), La(III), Eu(III), Yb(III), Zr(IV), Hf(IV) − 10:1 POM:GG 2.0 mM, 50 °C, pD 5.50 for Mn(III), Fe(III), Co(II), Ni(II), Cu(III)). The lack of reactivity observed for the POMs containing first row transition metal ions (Mn(III), Fe(III),

dx.doi.org/10.1021/ic301364n | Inorg. Chem. 2012, 51, 9902−9910

Co(II), Ni(II), and Cu(III)) can be explained by the coordination environment of the metal ion.[47,52] In these POMs the metal ion has a 6-fold octahedral coordination environment in which the polyoxometalate ligand acts as a pentadentate ligand. The sixth coordination site is occupied by water which can be substituted by other ligands.[47,52] However, previous studies have shown that effective hydrolysis of peptides usually requires the presence of at least two free coordination sites on the metal center: one for the attachment of the peptide and the other for the internal delivery of the water molecule which acts as an effective nucleophile.[53] In contrast to first row transition metals, rare earth ions are characterized by higher coordination numbers and after incorporation into the Wells–Dawson POM more free coordination sites around the metal ion are present. However, despite this fact, the Y(III), La(III), Eu(III), and Yb(III) substituted POMs showed low activity toward GG hydrolysis. This might be due to a decreased Lewis acidity resulting from incorporation into the POM structure[20] or due to the formation of dimeric POM species in solution.[48] On the other hand, Zr(IV) and Hf(IV) were active toward hydrolysis of the peptide bond in GG. At pD 7.2 and 50 °C 2.0 mM of glycylglycine was fully hydrolyzed in the presence of 2.0 mM of the Zr(IV)- and Hf(IV)-substituted Wells–Dawson type POM. Therefore the Zr(IV)-substituted Wells–Dawson POM $K_{15}H$-$[Zr(\alpha_2\text{-}P_2W_{17}O_{61})_2]\cdot 25H_2O$ (**1**) was selected to explore in detail this novel type of reactivity.

Aqueous Solution Behavior of 1. Incorporation of Zr(IV) into the monolacunary α_2-Wells–Dawson POM results in its coordination to four oxygen atoms in the vacancy of the POM. In contrast to other transition metal ions which are usually tetra- or hexa-coordinated, Zr(IV) shows higher coordination numbers. As a result, incorporation of Zr(IV) into the Wells–Dawson type POM results in the formation of a 1:2 species in which Zr(IV) is 8-coordinated. The singe crystal X-ray structure of **1** shows that one Zr(IV) ion coordinates two Wells–Dawson units.[46] This species is expected to have low catalytic activity in solution because of the absence of water molecules that can be replaced by the substrate in the coordination sphere of Zr(IV). However, when the 1:2 species is dissolved in water multiple equilibria between the dimeric 2:2, monomeric 1:1, and sandwich type 1:2 Zr(IV):POM complexes are observed, depending on the pH, temperature, and concentration (Scheme 1).[54−56] Among all the species present in solution, the 1:1 monomer is anticipated to have the most favorable catalytic properties because of several free coordination sites that are available for interaction with the substrate.[57]

Since all POMs shown in Scheme 1 are characterized by a specific ^{31}P NMR resonance, the species distribution at different solution conditions can be monitored by ^{31}P NMR spectroscopy. As can be seen from Figure 1 and Supporting Information, Figure S1 a decrease in the amount of 1:2 (characterized by ^{31}P NMR signals at −9.34 ppm and −13.95 ppm)[46] is observed when the pD is lowered. While at pD 7.0 the 1:2 sandwich type is the only species present in solution, at pD 3.0 the 1:1 monomer (characterized by ^{31}P NMR signals at −10.04 ppm and −13.76 ppm)[56] and the 1:2 species are present in a 70:30 ratio. At pD 1.5 only the 1:1 monomer is present. These data are consistent with a study performed by Nomiya et al.[54] In that study it was concluded that the acidification of an aqueous solution containing the 1:2 compound resulted in the formation of the 2:2 or 1:1 species, as well as the saturated Wells–Dawson POM $[\alpha\text{-}P_2W_{18}O_{62}]^{6-}$. The latter species was also observed in our study, and it was characterized by a single ^{31}P NMR resonance at −12.85 ppm. It can be concluded that lower pD values are expected to be beneficial for the catalytic activity of **1** since they favor the 1:1 species over the 1:2 complex. In the following step the influence of the starting concentration of **1** on the species distribution was investigated. Supporting Information, Figure S2 and Table S1 show the species distribution as a function of the initial concentration of **1** at pD 5.0. For a 10.0 mM solution of **1** only the ^{31}P NMR resonances of the 1:2 compound were observed. However, the presence of $[\alpha\text{-}P_2W_{18}O_{62}]^{6-}$ implies that a small fraction of the 1:2 compound is converted into the 1:1 species. While $[\alpha\text{-}P_2W_{18}O_{62}]^{6-}$ is characterized by two chemically equivalent P atoms, the 1:1 species consists of 2 nonequivalent P atoms resulting in a lower signal intensity and will therefore not be detected at low concentrations. While for an initial concentration of 2.0 mM of **1**, the 1:2 and 1:1 species were present in a 80:20 ratio, the inverse (20:80) is observed for a 0.5 mM solution. Therefore it can be concluded that low concentrations of **1** result in higher fractions of the desired 1:1 monomer. Samples containing 2.0 mM and 10.0 mM of **1** were kept at pD 5.0 and 60 °C for a prolonged period to investigate the species distribution as a function of time. Surprisingly, for the 2.0 mM sample, no 1:1 monomer was detected after 1 day. Instead, two resonances corresponding to the 2:2 species were

Scheme 1. Equilibria between the 2:2, 1:1, and 1:2 Zr(IV):POM Species

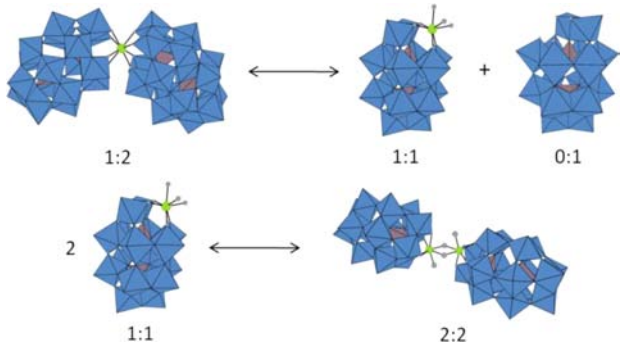

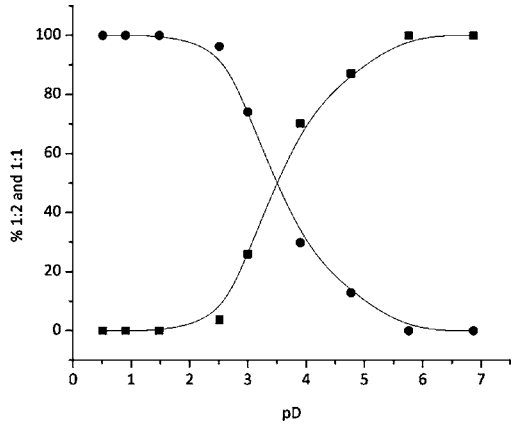

Figure 1. pD dependence of the distribution of 2.0 mM of **1** (1:2, solid squares, and 1:1, solid circles) obtained by ^{31}P NMR recorded immediately after mixing and pH adjustment.

dx.doi.org/10.1021/ic301364n | Inorg. Chem. 2012, 51, 9902−9910

observed. Over the course of several days the intensity of these signals increased, while the intensity of the 1:2 resonances decreased. Supporting Information, Table S2 summarizes the species distribution both for 2.0 mM and 10.0 mM of **1** as a function of reaction time at 60 °C. The data suggest that for both a 2.0 mM and 10.0 mM solution the equilibrium distribution between the 2:2 dimer and 1:2 species is obtained after 2 days at 60 °C. Interestingly, for the 2.0 mM solutions both species are present in a 50:50 ratio, while for 10.0 mM the 2:2 and 1:2 species are distributed in a 20:80 ratio. As the hydrolysis of peptide was monitored at elevated temperatures, the effect of temperature on the POM species distribution of a 2.0 mM solution of **1** at pD 5.0 was also examined (Supporting Information, Figure S3). At temperatures below 50 °C the 1:1 monomer and 1:2 species were detected. Above 70 °C only the 2:2 dimer and the 1:2 complex were present. For the 60 °C sample an intermediate distribution was observed. A chemical shift difference in between that of the 1:1 monomer and 2:2 dimer was obtained. The broadening of the resonance signal at −13.81 ppm confirmed the interchange between the 1:1 and 2:2 species.

Hydrolysis of Gly-Gly (GG). GG was fully hydrolyzed to glycine (G) in the presence of equimolar amounts of **1** at pD 5.0 and 60 °C. The reaction was followed by recording ^{1}H NMR spectra (Figure 2) at different reaction times. A gradual

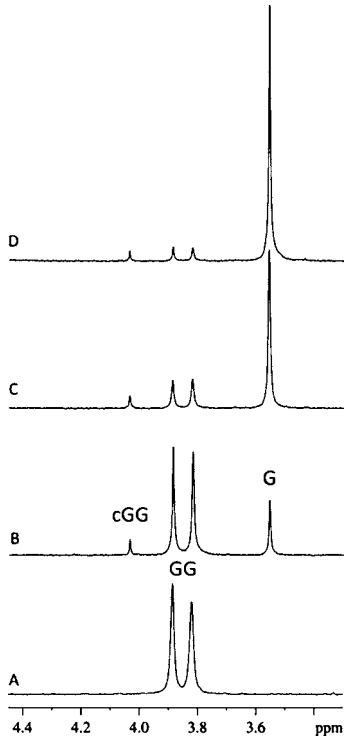

Figure 2. ^{1}H NMR spectra recorded at various reaction times during the hydrolysis of 2.0 mM of GG in the presence of 2.0 mM of **1** at pD 5.0 and 60 °C. (A) After mixing, (B) after 14 days, (C) after 24 days and (D) 23 days.

decrease of the two GG resonances at 3.82 ppm and 3.89 ppm and an increase of the G resonance at 3.56 ppm were observed over time. In addition, a fourth resonance at 4.04 ppm was detected in the course of the hydrolytic reaction. Several studies reporting the hydrolysis of dipeptides demonstrated that in addition to amide bond hydrolysis, diketopiperazine formation occurs.[43,58] Indeed, upon adding glycine anhydride (cGG) to the reaction mixture, an intensity increase of the resonance at 4.04 ppm was observed. This undoubtedly demonstrates that cyclization of GG also occurred in the presence of **1**. Figure 3

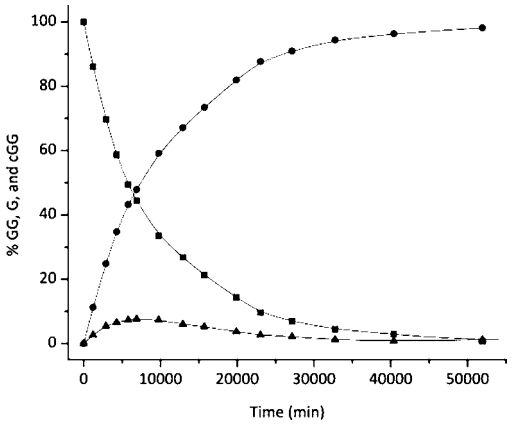

Figure 3. Hydrolysis of 2.0 mM of GG in the presence of 2.0 mM of **1** at pD 5.0 and 60 °C. Percentage of GG (solid squares), G (solid circles), and cGG (solid triangles) as a function of reaction time.

shows the percentage of GG, G, and cGG as a function of reaction time, calculated on the basis of the intensity of their ^{1}H NMR resonances. As can be seen from Figure 3, the amount of cGG reaches a maximum of 7.50%, before gradually decreasing to zero. However, since the kinetic experiments were performed immediately upon mixing **1** with GG it is possible that part of the cGG formation is correlated to the equilibration process of **1**.

No precipitation or turbidity was observed in any of the reactions with **1**, indicating that the Wells−Dawson POM ligand is able to stabilize Zr(IV) in aqueous solutions. The observed rate constant (k_{obs}) for the hydrolysis of GG was calculated by fitting the increase in the concentration of G to a monoexponential function. Its value, k_{obs} = 9.2 (±0.2) × 10^{-5} min^{-1} ($t_{1/2}$ = 5 days) represents a significant acceleration compared to the blank reaction. In the absence of **1** no hydrolysis of the amide bond in GG was observed after two months at 60 °C. Therefore it is difficult to precisely calculate the rate acceleration compared to the uncatalyzed cleavage. However, based on literature data, a half-life of about 5 years was estimated for the uncatalyzed reaction under similar conditions.[34] No hydrolysis was observed in the presence of the lacunary $[\alpha_2\text{-}P_2W_{17}O_{61}]^{10-}$, implying that the presence of Zr(IV) is essential for the hydrolytic activity. The hydrolysis of 2.0 mM of GG in the presence of 2.0 mM of $ZrCl_4$ was also studied at pD 5.0 and 60 °C and while after about 4 days free glycine was observed in ^{1}H NMR, the data were difficult to quantify as the reaction mixture was not homogeneous because of gel formation. This is consistent with the previous studies investigating the aqueous solution behavior of Zr(IV) in which the formation of polymeric $[Zr_8(OH)_{20}(H_2O)_{24}]^{12+}$ species upon dissolving Zr(IV) in aqueous solutions was observed.[59]

The disappearance of the cGG peak suggests that **1** promotes its formation but also its hydrolysis. The reversibility of diketopiperazine formation was examined by following the hydrolysis of 2.0 mM of cGG (Supporting Information, Figure S4) in the presence of 2.0 mM of **1** at pD 5.0 and 60 °C. As can be seen from Supporting Information, Figure S5 the addition of **1** to cGG resulted in complete conversion of cGG into G.

dx.doi.org/10.1021/ic301364n | Inorg. Chem. 2012, 51, 9902−9910

However, an induction period for the formation of G was observed (inset Supporting Information, Figure S5) as hydrolysis to G could only be observed after sufficient amounts of GG were formed, suggesting that GG acts as an intermediate in the conversion of cGG to G. This is not surprising since hydrolysis of cGG to G would require the breaking of two chemical bonds at the same time. As it was the case for GG, no hydrolysis in the presence of $[\alpha_2\text{-}P_2W_{17}O_{61}]^{10-}$ was detected. Additionally, no conversion to GG, followed by hydrolysis to G, was observed in the absence of **1**. On the basis of these observations, we propose the reaction scheme presented in Scheme 2.

Scheme 2. Hydrolysis of GG in the Presence of 1

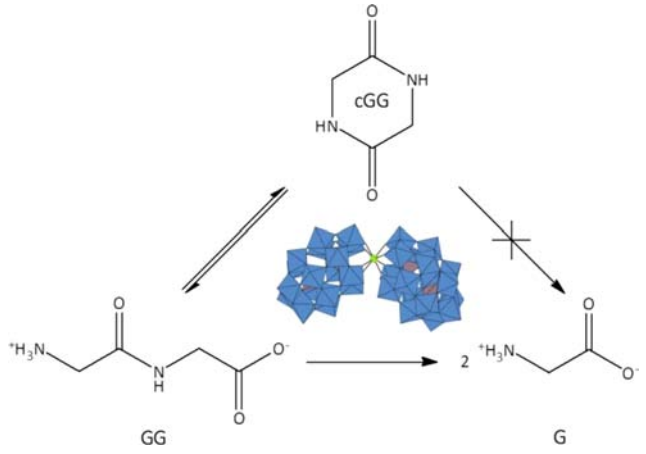

The effect of salt ions on k_{obs} was investigated by adding LiCl to a reaction mixture containing 2.0 mM of GG and 2.0 mM of **1**. Supporting Information, Figure S6 shows that upon adding increasing amounts of LiCl the hydrolysis rate constant decreased. In the presence of 1.0 M of LiCl, a 3-fold decrease in k_{obs} was observed. This results in an increase in half-life from 5 to 15 days. The presence of LiCl could influence the POM speciation or affect the electrostatic interaction between **1** and GG. To differentiate between these two possibilities, the speciation of **1** in the presence of LiCl was further examined. ^{31}P NMR results show that increasing the LiCl concentration up to 1.0 M did not change the solution speciation of **1** and point toward the importance of electrostatic interactions for the effective hydrolysis of GG.

The reaction between 2.0 mM of GG and 2.0 mM of **1** was also studied at various temperatures at pD 5.0 (Supporting Information, Figure S7). Increasing the reaction temperature from 37 to 80 °C resulted in a 100-fold increase of the reaction rate constant and a decrease of the half-life to 0.5 days. When the data in Supporting Information, Figure S7 were fitted to the Arrhenius equation both the pre-exponential factor, 1.6 $(\pm 0.4)\cdot 10^{13}$ min^{-1}, and the experimentally determined activation energy, 91.0 ($\pm$0.7) kJ mol^{-1}, were obtained. Comparison of the obtained activation energy to the one in the absence of any catalyst is difficult since very few reports on the activation energy for hydrolysis of dipeptides are available. However, high temperature studies on the natural hydrolysis of GG at near neutral pH resulted in an estimation of 96 kJ mol^{-1} for the conversion of GG to G+G.[34] This implies that in the presence of **1** the activation energy for the hydrolysis of GG is lowered by 3−5 kJ mol^{-1}. Linear fitting of $\ln(k_{obs}/T)$ as a function of the reciprocal temperature to the Eyring equation (Supporting Information, Figure S8) allows for the calculation of the enthalpy of activation, $\Delta H^{\ddagger}$ = 96.14 kJ mol^{-1}, and entropy of activation, $\Delta S^{\ddagger}$ = −33.53 J mol^{-1} K^{-1}. At 60 °C the Gibbs free energy of activation is 107.31 kJ mol^{-1}. The negative value of $\Delta S^{\ddagger}$ is the result of the coordination of GG to the metal center.

Hydrolysis of Gly-Gly Derivatives. The influence of **1** on the hydrolysis of several GG derivatives was investigated to get more insight in the binding mode of GG to **1**. For this purpose GG derivatives that were modified at the N- and C-terminal end were prepared. Figure 4 gives an overview of the substrates that were investigated.

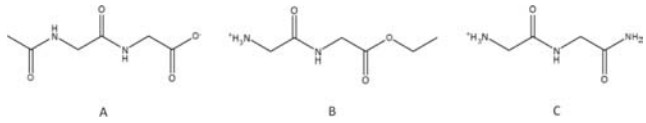

Figure 4. (A) acetamidoglycylglycinate (AcGG), (B) ethyl glycylglycinate (GGOEt), and (C) glycylglycyl amide ($GGNH_2$).

^{1}H NMR spectra of a solution containing 2.0 mM of acetamidoglycylglycinate (AcGG) in the presence of 2.0 mM of **1** did not show any evidence of amide bond hydrolysis after 7 days at pD 5.0 and 60 °C. This suggests that the free amino-terminus is of importance for the interaction of the substrate with the POM. The interaction may occur via coordination to the metal center or via secondary interactions of the protonated amino group with the negatively charged surface of **1**. When ethyl glycylglycinate (GGOEt) was used, full hydrolysis of the ethyl ester bond was observed within a few hours prior to amide bond hydrolysis. ^{1}H NMR spectra clearly indicate the formation of ethanol in the beginning of the reaction. Once all GGOEt was converted to GG a similar hydrolysis profile to that of GG was observed (Supporting Information, Figure S9). In the absence of **1**, no hydrolysis of both the ester and the amide bond was observed after 5 days at 60 °C and pD 5.0. For glycylglycyl amide ($GGNH_2$), hydrolysis of the C-terminal amide functionality resulted in the formation of GG. This process was slow compared to ester bond hydrolysis in GGOEt, and as can be seen from Supporting Information, Figure S10 hydrolysis of GG occurred before all $GGNH_2$ was converted into GG. No free glycine amide (GNH_2) was detected during the course of the reaction indicating that the hydrolysis of the terminal G-NH_2 amide bond occurs preferentially to internal G-G amide bond hydrolysis in $GGNH_2$.

Peptide Binding to 1. ^{13}C NMR studies (Figure 5 and Table 1) performed on the mixture of GG with **1** suggest that both carbonyl functionalities of GG interact with **1**, with the largest shift being observed for the amide carbonyl. This is

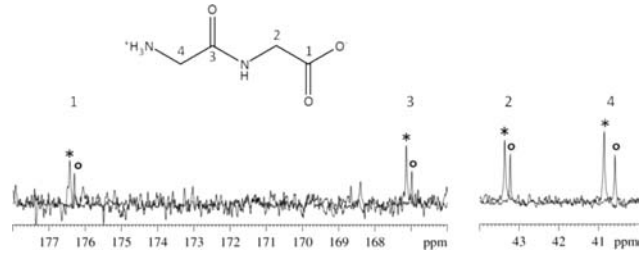

Figure 5. ^{13}C NMR spectrum of GG in the presence (*) and absence (°) of **1**.

dx.doi.org/10.1021/ic301364n | Inorg. Chem. 2012, 51, 9902−9910

Table 1. ^{13}C NMR Chemical Shift Values (ppm) of GG in the Presence and Absence of 1

	30.0 mM GG	10.0 mM GG + 10.0 mM 1	Δ(ppm)
C1(CO)	176.30	176.42	0.12
C3(CO)	166.93	167.14	0.16
C2(CH_2)	43.23	43.36	0.13
C4(CH_2)	40.58	40.86	0.28

important since coordination of the amide carbonyl to Zr(IV) facilitates amide bond hydrolysis by activating the amide carbon toward nucleophilic attack by water molecules. As a result of this coordination the ^{13}C NMR resonance of the methylene group adjacent to the amide carbonyl experienced the largest shift. This shift is also consistent with the observation that the N-terminal amine functionality plays on important role in the coordination, and is consistent with the lack of hydrolysis observed in AcGG, a N-terminal blocked derivative of GG. The C-terminal carbonyl carbon also experienced a shift. However this shift appears not to be the result of interaction of GG with the Zr(IV) center in **1**. Coordination of GG via its amine nitrogen and carbonyl amide oxygen renders coordination of the C-terminal carbonyl group sterically impossible because of the geometrical constraints imposed by the energetically favored trans configuration of the amide bond. The observed shift is most likely the result of a concentration effect observed for the ^{13}C NMR shift values of a pure GG solution. When the ^{13}C NMR shifts of a 10.0 mM solution of GG were compared to those of a 30.0 mM solution of GG all carbon atoms had identical chemical shift values except for the C-terminal carbonyl carbon. A difference of 0.12 ppm, similar to the one in the presence of **1**, was observed and is most likely caused by the intermolecular hydrogen bonding that occurs in peptide solutions.[60] These observations led us to propose that the coordination of Zr(IV) occurs via the amine nitrogen atom and amide oxygen. In a next step the binding of AcGG to **1** was examined. As can be seen from Supporting Information, Figure S11 and Table S3, only the resonances corresponding to the C-terminal carboxyl group and the adjacent methylene group are significantly shifted. In contrast to GG, no coordination of the amide carbonyl is observed. This mode of coordination is not favorable for the activation of the amide bond toward hydrolysis and may explain the lack of reactivity of **1** toward AcGG.

For GGOEt the biggest shifts are observed for the amide carbonyl and the adjacent methylene group (Supporting Information, Figure S12 and Table S4). Coordination of the ester carbonyl oxygen atom explains the ester bond hydrolysis observed during the first hours of reaction. Despite the smaller shift after the addition of **1**, ester bond hydrolysis proceeded at a significantly higher reaction rate compared to amide bond hydrolysis. This is because ester bonds are more kinetically labile and more susceptible toward hydrolysis compared to peptide bonds.

pD Dependence of k_{obs}. The pD dependence of the GG hydrolysis rate constant (Figure 6) shows a bell-shape profile with a maximum at pD 5.0. When the pD was decreased from 8.0 to 5.0, an increase in k_{obs} was observed, while below pD 5.0 a decrease of k_{obs} was evidenced. This bell-shape like behavior is a typical sign of two opposing effects influencing k_{obs}. The reaction rate increase observed can be related to the aqueous solution species distribution diagram shown in Figure 1. It was shown that the 1:1 monomer content increased when the pD is

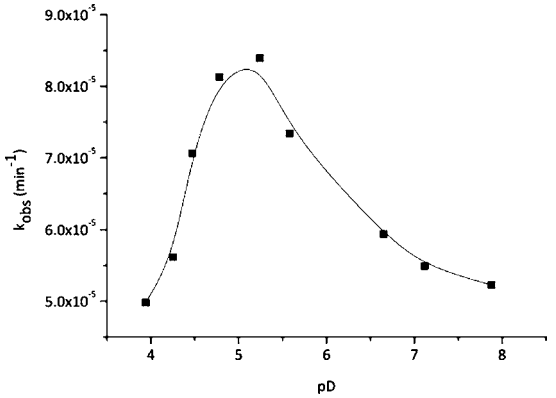

Figure 6. pD dependence of the rate constant for the hydrolysis of 2.0 mM of GG in the presence of 2.0 mM of **1** at 60 °C (solid squares).

lowered from 7.0 to 0.5. In the 1:1 species Zr(IV) is coordinated to 3 water molecules that can be replaced by GG. This makes the 1:1 species structurally most suitable for catalytic activity, and therefore an increase of its concentration results in a rate constant increase. However, at pD values lower than 5.0, where the 1:1 species is becoming the most abundant species, a reaction rate decrease is observed. This can be explained by the fact that coordination of the N-terminal amine group to the Zr(IV) center in GG requires the Zr(IV)-assisted deprotonation of the amine group. Since this process is impeded when the pD is decreased, a weaker interaction between GG and **1** is expected at lower pD-values resulting in a decrease of k_{obs}. Since the maximum rate was observed at pD 5.0, all further experiments were performed at this pD.

Catalytic Turnover. Figure 7 shows the influence of the concentration of **1** on the rate constant for the hydrolysis of 2.0

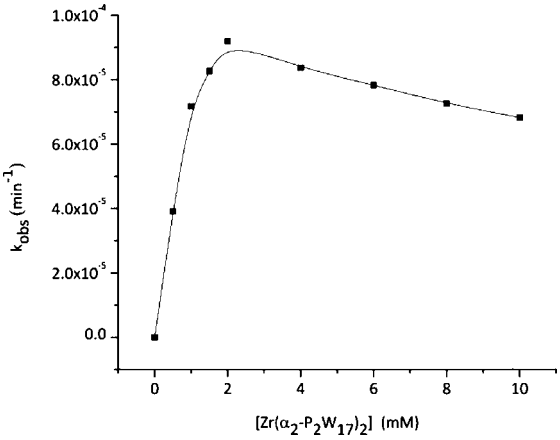

Figure 7. Influence of the concentration of **1** on the rate constant for the hydrolysis of 2.0 mM of GG at pD 5.0 and 60 °C.

mM of GG at pD 5.0 and 60 °C. These concentration studies revealed that **1** is not only able to significantly accelerate GG hydrolysis, but is also capable of hydrolyzing a larger molar excess of GG. In the presence of 0.2 mM of **1**, 2.0 mM of GG was completely hydrolyzed to G. Although modest, this turnover of 10 proves the principles of catalysis. The highest rate constant was obtained when GG and **1** were present in a 1:1 (2.0 mM) ratio. When more than 2.0 mM of **1** was used, a decrease in k_{obs} was observed. This finding can be explained keeping in mind both the concentration and the time

dx.doi.org/10.1021/ic301364n | Inorg. Chem. 2012, 51, 9902−9910

dependence of the equilibria. For a 10.0 mM sample of **1**, only the 1:2 species was present after dissolving **1** and pD adjustment to pD 5.0. However, when the sample was kept at 60 °C for several days, the 2:2 dimer was formed in a 20:80 ratio compared to the 1:2 species. For the 2.0 mM sample on the other hand, 20% of the 1:1 monomer and 80% of the 1:2 species were present after dissolving and pD adjustment to pD 5.0, and a 50:50 ratio of the 2:2 dimer compared to the 1:2 species was observed after a few days at 60 °C. Therefore, the decrease in concentration of the 2:2 dimer, in which Zr(IV) has free coordination sites available for the binding of GG, explains slower reaction rates observed upon increasing the concentration of **1** from 2.0 mM to 10.0 mM.

Inhibition Studies. To gain more insight into the coordination of GG to **1**, the hydrolysis of GG in the presence of several nonreactive substrate analogues was examined. To achieve efficient coordination of the inhibitor with the metal center, dicarboxylic acids with varying aliphatic chain lengths were chosen as candidates for inhibition experiments. In addition, malic and citric acid were also examined. These inhibitors are known to act as multidendate ligands for many metal ions (Figure 8).[61]

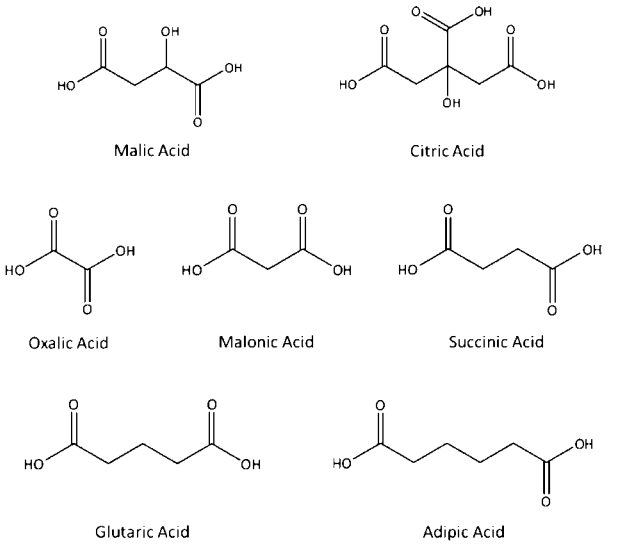

Figure 8. Chemical structure of the inhibitors used in this study.

Table 2 gives an overview of the rate constants for the hydrolysis of GG in the presence of the inhibitor. Malic and citric acid fully inhibited the hydrolysis of GG, while for the dicarboxylic acids a decrease of the reaction rate constant was observed depending on the length of the aliphatic chain. The largest effect was observed in the presence of oxalic acid, where no hydrolysis was observed. While malonic and glutaric acid strongly inhibited hydrolysis, the inhibition effect was much smaller in the presence of succinic and adipic acid. Coordination of the three carboxylate groups of citric acid to Zr(IV) most likely prevents the binding and Lewis acid activation of GG. For the dicarboxylic acids, it was assumed that when the aliphatic chain length was increased, the binding affinity of the inhibitor decreased most likely because of the formation of a larger, more flexible chelate ring. However, the hydrolysis rate constant measured in the presence of glutaric acid did not follow the proposed trend. When the structure of succinic acid is compared to that of malic acid, it can be seen that the only difference is the presence of an additional hydroxyl group in malic acid. The presence of this hydroxyl group is apparently responsible for the significant difference in inhibitory effect observed between these two acids. The tridendate coordination between malic acid and the 1:1 monomer was earlier observed by Fedin et al.[56] This study shows that carbonyl groups efficiently bind to the Zr(IV) center in **1**. This is important since the coordination of GG to **1** and its activation toward nucleophilic attack is mainly governed by carbonyl group interaction.

Table 2. Hydrolysis of 2.0 mM of GG in the Presence of 2.0 mM of 1 and 20.0 mM of the Inhibitor at pD 5.0 and 60 °C

inhibitor	no. of CH_2 groups	k_{obs} (min^{-1})
no inhibitor		9.2 (±0.2)·× 10^{-5}
oxalic acid	0	no hydrolysis
malonic acid	1	1.76 (±0.05)·× 10^{-5}
succinic acid	2	7.3 (±0.2)·× 10^{-5}
glutaric acid	3	4.0 (±0.2)·× 10^{-5}
adipic acid	4	9.7 (±0.4)·× 10^{-5}
malic acid		no hydrolysis
citric Acid		no hydrolysis

Hydrolysis Mechanism. ^{13}C NMR interaction studies and inhibition experiments show that the amide carbonyl plays a vital role in the coordination of GG to the Zr(IV) ion in **1**. Coordination of the amide carbonyl leads to Lewis acid activation of the amide bond and makes it more susceptible toward nucleophilic attack by water resulting in the hydrolysis of GG (Scheme 3). Both the attack of coordinated water, which is an internal nucleophile, and that of solvent water are possible and these two mechanisms are kinetically indistinguishable.[35] The N-terminal amine group is considered as the second coordinating entity, which seems to be essential for the effective attachment of the peptide as the N-blocked analogue AcGG was not hydrolyzed in the presence of **1**.

Scheme 3. Mechanism for the Hydrolysis of GG in the Presence of 1: Nucleophilic Attack of Solvent Water (Left) and Coordinated Water (Right)

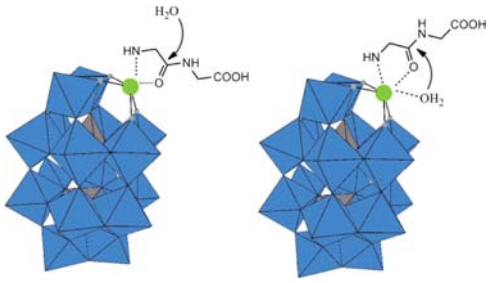

Hydrolysis of Other Dipeptides. The reactivity of **1** toward other dipeptides with a Gly-X sequence was examined, where X = Ala, Val, Leu, Ile, Phe, Ser, Thr, Tyr, Glu, Gln, Asn, Asp, His, Lys, Arg, Met, and Cys. All dipeptides were fully hydrolyzed, and we are currently investigating the dependence of the rate constant on the nature of the X side chain. For example Gly-Ser was hydrolyzed at a significantly higher rate (k_{obs} = 2.08 × 10^{-4} min^{-1} at pD 5.0 and 60 °C) as compared to Gly-Gly, because of an intramolecular N→O acyl rearrangement which leads to peptide bond hydrolysis.[41] Dipeptides containing bulky residues such as Gly-Leu were hydrolyzed much slower (k_{obs} = 8.56 × 10^{-6} min^{-1}) presumably because of

dx.doi.org/10.1021/ic301364n | Inorg. Chem. 2012, 51, 9902−9910

the steric hindrance of the side chain of the Leu residue, which prevents effective delivery of the nucleophile. A more detailed study on the hydrolysis of dipeptides by **1** is currently underway.

Hydrolysis of Triglycine, Tetraglycine, and Pentaglycine. The hydrolytic activity of **1** was further tested on longer peptides consisting of glycine residues. Supporting Information, Figure S13 shows the assignment of the ^{1}H NMR spectra recorded during the hydrolysis of triglycine (3G) in the presence of **1**. Quantitative analysis of these spectra was made possible since each reactant (except for cGG) was characterized by at least one isolated ^{1}H NMR resonance. The kinetic profile of the species observed during the course of hydrolytic reaction is shown in Supporting Information, Figure S14. GG and G were formed in equal amounts in the early stages of the reaction. Once GG is formed, parallel pathways in which 3G and GG are hydrolyzed can occur. Interestingly, the hydrolysis of GG into G occurred before all 3G was converted to GG. Furthermore, cyclization of GG to cGG was observed. Eventually, all 3G was fully converted to G. Figure 9 shows

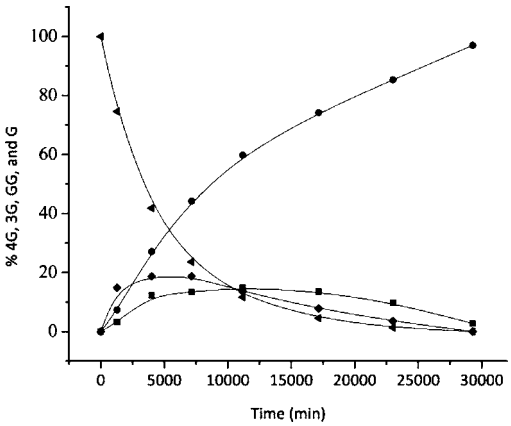

Figure 9. Hydrolysis of 2.0 mM of 4G in the presence of 2.0 mM of **1** at pD 5.0 and 60 °C. Percentage of 4G (left pointing solid triangles), 3G (solid diamonds), GG (solid squares), and G (solid circles) as a function of reaction time.

the time dependence of the distribution of all species that were present during the hydrolysis of 2.0 mM of tetraglycine (4G) in the presence of 2.0 mM of **1** at 60 °C and pD 5.0. For the hydrolysis of 4G an induction period for the formation of GG was observed. Initially only conversion of 4G to 3G+G was detected. An alternative pathway would be the conversion of 4G to GG+GG. Since no GG was observed during the first 24 h of reaction, it can be concluded that **1** shows exopeptidase rather than endopeptidase reactivity. This is further confirmed by the relative position of the percentage maxima of 3G and GG. Whereas the maximum amount of 3G is present after 3 days, the maximum in GG concentration was only observed after 8 days. At the end of reaction a full conversion of 4G into G was observed.

A detailed analysis of the ^{1}H NMR spectra recorded during the hydrolysis of 2.0 mM of pentaglycine (5G) in the presence of 2.0 mM of **1** at pD 5.0 and 60 °C was not possible because of the complexity of the ^{1}H NMR spectra. However, ^{1}H NMR spectra recorded at various reaction times clearly indicated the full conversion of 5G to G, which at the end of the reaction was the sole product of hydrolysis.

Supporting Information, Figure S15 and Table S5 summarize the ^{13}C chemical shifts of 3G both in the presence and in the absence of **1**. Both amide carbonyls and corresponding methylene groups displayed the biggest shift. On the basis of the ^{13}C chemical shift values for 4G, reported in Supporting Information, Figure S16 and Table S6, the assumption that **1** displays exo- rather than endopeptidase activity cannot be validated. In the case of exopeptidase activity a clear preference for coordination to amide carbon 3 and/or 7 is expected. Since all three amide carbons display a significant shift in the presence of **1** no distinction between exo- and endopeptidase activity can be made. Instead, 4G might act as a bridging ligand between two POMs or display multiple coordination modes to Zr(IV). The insolubility of 5G at concentrations (10.0 mM) needed for ^{13}C NMR made a ^{13}C NMR study of the binding of 5G to **1** impossible.

CONCLUSIONS

Homogeneous hydrolysis of the highly inert amide bond in the dipeptide glycylglycine was observed in the presence of the Zr(IV)-substituted Wells−Dawson type POM. The hydrolysis rate constant represents a significant acceleration compared to the blank reaction in which no hydrolysis was observed after several months under the same reaction conditions. Several dipeptides and oligopeptides were also successfully hydrolyzed by **1**, demonstrating that the catalyst can be applied to a range of different peptide bond containing substrates. The hydrolytic activity of the POM toward proteins is currently under investigation, with the ultimate goal of developing metal-substituted POMs as a novel class of artificial proteases.

ASSOCIATED CONTENT

Supporting Information

^{1}H, ^{13}C, and ^{31}P NMR data. This material is available free of charge via the Internet at http://pubs.acs.org.

AUTHOR INFORMATION

Corresponding Author

*E-mail: Tatjana.Vogt@chem.kuleuven.be.

Notes

The authors declare no competing financial interest.

ACKNOWLEDGMENTS

G.A. thanks the FWO-Flanders (Belgium) for the postdoctoral fellowship. T.N.P.-V. acknowledges KU Leuven for the financial support (Research Fund START1/09/028).

REFERENCES

(1) Borras-Almenar, J. J.; Coronado, E.; Muller, A.; Pope, M. T. *Polyoxometalate molecular science*; Kluwer Academic Publishers: Dordrecht, The Netherlands, 2003.
(2) Rhule, J. T.; Hill, C. L.; Judd, D. A. *Chem. Rev.* **1998**, *98*, 327.
(3) Yamase, T. *J. Mater. Chem.* **2005**, *15*, 4773.
(4) Kozhevnikov, I. *Catalysis by polyoxometalates*; John Wiley & Sons, Ltd: Chichester, U.K., 2002; Vol. *2*.
(5) Mizuno, N.; Kamata, K.; Yamaguchi, K. *Top. Catal.* **2010**, *53*, 876.
(6) Mizuno, N.; Yamaguchi, K.; Kamata, K. *Coord. Chem. Rev.* **2005**, *249*, 1944.
(7) Estrada, A. C.; Santos, I. C. M. S.; Simoes, M. M. Q.; Neves, M. G. P. M. S.; Cavaleiro, J. A. S.; Cavaleiro, A. M. V. *Appl. Catal., A* **2011**, *392*, 28.
(8) Mizuno, N.; Nozaki, C.; Kiyoto, I.; Misono, M. *J. Am. Chem. Soc.* **1998**, *120*, 9267.

(9) Mizuno, N.; Nozaki, C.; Kiyoto, I.; Misono, M. *J. Catal.* **1999**, *182*, 285.
(10) Chen, F. W.; Dong, T.; Li, X. F.; Xu, T. G.; Hu, C. W. *Chin. Chem. Lett.* **2011**, *22*, 871.
(11) Jiang, C. J.; Guo, Y. H.; Wang, C. G.; Hu, C. W.; Wu, Y.; Wang, E. B. *Appl. Catal., A* **2003**, *256*, 203.
(12) Yasuda, H.; He, L. N.; Sakakura, T.; Hu, C. W. *J. Catal.* **2005**, *233*, 119.
(13) Sartorel, A.; Carraro, M.; Scorrano, G.; Bassil, B. S.; Dickman, M. H.; Keita, B.; Nadjo, L.; Kortz, U.; Bonchio, M. *Chem.—Eur. J.* **2009**, *15*, 7854.
(14) Orlandi, M.; Argazzi, R.; Sartorel, A.; Carraro, M.; Scorrano, G.; Bonchio, M.; Scandola, F. *Chem. Commun.* **2010**, *46*, 3152.
(15) Kholdeeva, O. A.; Maksimov, G. M.; Maksimovskaya, R. I.; Vanina, M. P.; Trubitsina, T. A.; Naumov, D. Y.; Kolesov, B. A.; Antonova, N. S.; Carbo, J. J.; Poblet, J. M. *Inorg. Chem.* **2006**, *45*, 7224.
(16) Kholdeeva, O. A.; Maksimovskaya, R. I. *J. Mol. Catal. A: Chem.* **2007**, *262*, 7.
(17) Al-Kadamany, G.; Mal, S. S.; Milev, B.; Donoeva, B. G.; Maksimovskaya, R. I.; Kholdeeva, O. A.; Kortz, U. *Chem.—Eur. J.* **2010**, *16*, 11797.
(18) Jahier, C.; Mal, S. S.; Kortz, U.; Nlate, S. *Eur. J. Inorg. Chem.* **2010**, 1559.
(19) Carraro, M.; Nsouli, N.; Oelrich, H.; Sartorel, A.; Soraru, A.; Mal, S. S.; Scorrano, G.; Walder, L.; Kortz, U.; Bonchio, M. *Chem.—Eur. J.* **2011**, *17*, 8371.
(20) Boglio, C.; Lemiere, G.; Hasenknopf, B.; Thorimbert, S.; Lacote, E.; Malacria, M. *Angew. Chem., Int. Ed.* **2006**, *45*, 3324.
(21) Boglio, C.; Micoine, K.; Remy, P.; Hasenknopf, B.; Thorimbert, S.; Lacote, E.; Malacria, M.; Afonso, C.; Tabet, J. C. *Chem.—Eur. J.* **2007**, *13*, 5426.
(22) Kikukawa, Y.; Yamaguchi, S.; Nakagawa, Y.; Uehara, K.; Uchida, S.; Yamaguchi, K.; Mizuno, N. *J. Am. Chem. Soc.* **2008**, *130*, 15872.
(23) Kikukawa, Y.; Yamaguchi, S.; Tsuchida, K.; Nakagawa, Y.; Uehara, K.; Yamaguchi, K.; Mizuno, N. *J. Am. Chem. Soc.* **2008**, *130*, 5472.
(24) Cartuyvels, E.; Absillis, G.; Parac-Vogt, T. N. *Chem. Commun.* **2008**, 85.
(25) Absillis, G.; Cartuyvels, E.; Van Deun, R.; Parac-Vogt, T. N. *J. Am. Chem. Soc.* **2008**, *130*, 17400.
(26) Steens, N.; Ramadan, A. M.; Absillis, G.; Parac-Vogt, T. N. *Dalton Trans.* **2010**, *39*, 585.
(27) Absillis, G.; Van Deun, R.; Parac-Vogt, T. N. *Inorg. Chem.* **2011**, *50*, 11552.
(28) Van Lokeren, L.; Cartuyvels, E.; Absillis, G.; Willem, R.; Parac-Vogt, T. N. *Chem. Commun.* **2008**, 2774.
(29) Cartuyvels, E.; Van Hecke, K.; Van Meervelt, L.; Gorller-Walrand, C.; Parac-Vogt, T. N. *J. Inorg. Biochem.* **2008**, *102*, 1589.
(30) Steens, N.; Ramadan, A. M.; Parac-Vogt, T. N. *Chem. Commun.* **2009**, 965.
(31) Ho, P. H.; Breynaert, E.; Kirschhock, C. E. A.; Parac-Vogt, T. N. *Dalton Trans.* **2011**, *40*, 295.
(32) (a) Ho, P. H.; Stroobants, K.; Parac-Vogt, T. N. *Inorg. Chem.* **2011**, *50*, 12025. (b) Ho, P. H.; Mihaylov, T.; Pierloot, K.; Parac-Vogt, T. N. *Inorg. Chem.* **2012**, *51*, 8848.
(33) Zhang, G. J.; Keita, B.; Craescu, C. T.; Miron, S.; de Oliveira, P.; Nadjo, L. *Biomacromolecules* **2008**, *9*, 812.
(34) Radzicka, A.; Wolfenden, R. *J. Am. Chem. Soc.* **1996**, *118*, 6105.
(35) Grant, K. B.; Kassai, M. *Curr. Org. Chem.* **2006**, *10*, 1035.
(36) Parac, T. N.; Kostic, N. M. *J. Am. Chem. Soc.* **1996**, *118*, 5946.
(37) Milovic, N. M.; Dutca, L. M.; Kostic, N. M. *Chem.—Eur. J.* **2003**, *9*, 5097.
(38) Kopera, E.; Krezel, A.; Protas, A. M.; Belczyk, A.; Bonna, A.; Wyslouch-Cieszynska, A.; Poznanski, J.; Bal, W. *Inorg. Chem.* **2010**, *49*, 6636.
(39) Suh, J. *Acc. Chem. Res.* **2003**, *36*, 562.
(40) Kassai, M.; Grant, K. B. *Inorg. Chem. Commun.* **2008**, *11*, 521.
(41) Yashiro, M.; Sonobe, Y.; Yamamura, A.; Takarada, T.; Komiyama, M.; Fujii, Y. *Org. Biomol. Chem.* **2003**, *1*, 629.
(42) Buckingham, D. A.; Clark, C. R. In *Probing of Proteins by Metal Ions and Their Low-Molecular-Weight Complexes*; Marcel Dekker: New York, 2001; Vol. *38*, p 43.
(43) Takarada, T.; Yashiro, M.; Komiyama, M. *Chem.—Eur. J.* **2000**, *6*, 3906.
(44) Kassai, M.; Ravi, R. G.; Shealy, S. J.; Grant, K. B. *Inorg. Chem.* **2004**, *43*, 6130.
(45) Vanhaecht, S.; Absillis, G.; Parac-Vogt, T. N. *Dalton Trans.* **2012**, *41* (7), 10018.
(46) Kato, C. N.; Shinohara, A.; Hayashi, K.; Nomiya, K. *Inorg. Chem.* **2006**, *45*, 8108.
(47) Lyon, D. K.; Miller, W. K.; Novet, T.; Domaille, P. J.; Evitt, E.; Johnson, D. C.; Finke, R. G. *J. Am. Chem. Soc.* **1991**, *113*, 7209.
(48) Zhang, C.; Bensaid, L.; McGregor, D.; Fang, X. F.; Howell, R. C.; Burton-Pye, B.; Luo, Q. H.; Todaro, L.; Francesconi, L. C. *J. Clust. Sci.* **2006**, *17*, 389.
(49) Vaidya, A. A.; Lele, B. S.; Kulkarni, M. G.; Mashelkar, R. A. Vol. U. S. Patent 6605714, 2003.
(50) Odonnell, M. J.; Burkholder, T. P.; Khau, V. V.; Roeske, R. W.; Tian, Z. *Pol. J. Chem.* **1994**, *68*, 2477.
(51) Covingto., Ak; Paabo, M.; Robinson, R. A.; Bates, R. G. *Anal. Chem.* **1968**, *40*, 700.
(52) Weakley, T. J. R. *Polyhedron* **1987**, *6*, 931.
(53) Parac, T. N.; Ullmann, G. M.; Kostic, N. M. *J. Am. Chem. Soc.* **1999**, *121*, 3127.
(54) Saku, Y.; Sakai, Y.; Nomiya, K. *Inorg. Chim. Acta* **2010**, *363*, 967.
(55) Sokolov, M. N.; Izarova, N. V.; Peresypkina, E. V.; Virovets, A. V.; Fedin, V. P. *Russ. Chem. Bull.* **2009**, *58*, 507.
(56) Sokolov, M. N.; Izarova, N. V.; Peresypkina, E. V.; Mainichev, D. A.; Fedin, V. P. *Inorg. Chim. Acta* **2009**, *362*, 3756.
(57) Dupre, N.; Remy, P.; Micoine, K.; Boglio, C.; Thorimbert, S.; Lacote, E.; Hasenknopf, B.; Malacria, M. *Chem.—Eur. J.* **2010**, *16*, 7256.
(58) Testa, B.; Mayer, J. M. *Hydrolysis in Drug and Prodrug Metabolism*; Wiley-VCH: Weinheim, Germany, 2003.
(59) Singhal, A.; Toth, L. M.; Lin, J. S.; Affholter, K. *J. Am. Chem. Soc.* **1996**, *118*, 11529.
(60) Nagaoka, S.; Terao, T.; Imashiro, F.; Saika, A.; Hirota, N.; Hayashi, S. *J. Chem. Phys.* **1983**, *79*, 4694.
(61) Strathmann, T. J.; Myneni, S. C. B. *Geochim. Cosmochim. Acta* **2004**, *68*, 3441.